Geometrically driven wrinkling observed in free plastic sheets and leaves

Eran Sharon
The Racah Institute of Physics, The Hebrew University of Jerusalem, Jerusalem 91904, Israel

Benoît Roman
Physique et Mécanique des Milieux Hétérogènes, UMR 7636 CNRS/ESPCI/Paris 6/Paris 7, 10 rue Vauquelin, 75231 cedex 5 Paris, France

Harry L. Swinney
Center for Nonlinear Dynamics and Department of Physics, University of Texas at Austin, Austin, Texas 78712, USA
(Received 28 July 2006; published 24 April 2007)

We have measured the multiscale wrinkling that occurs along the edge of torn plastic sheets. The plastic deformations produced by tearing define a new metric on the sheet, which then relaxes elastically. The resultant patterns of wrinkles correspond to a superposition of waves of different wavelengths. Measurements of the variation of the pattern as a function of the distance from the edge reveal a set of transitions, each of which adds a new mode to the cascade. The wavelengths λ in the cascade depend on both a geometrical length scale L_{geo} given by the metric near the sheet's edge, and the sheet thickness t: $\lambda \propto t^{0.3} L_{geo}^{0.7}$. This scaling implies vanishingly short wavelengths in the limit $t \to 0$. A possible geometrical origin of this behavior is discussed. Finally, we show that our measurement and analysis techniques are applicable to the study of some wavy patterns of leaves. These measurements reveal that the intrinsic geometry of a wavy leaf resembles that of the torn plastic sheets. This supports the possibility that some leaves form waves through a spontaneous wrinkling, rather than through an explicit three-dimensional construction.

DOI: 10.1103/PhysRevE.75.046211 PACS number(s): 89.75.Kd, 46.32.+x, 46.70.De

I. INTRODUCTION

Thin elastic sheets are common in nature. Thin sheets can be easily bent but they are relatively rigid against in-plane stretching and compression. This difference in rigidity is associated with the different scaling of the stretching and bending terms in the (Föppl-von Kármán) elastic energy functional of a sheet [1]. The stretching term is linear with the sheet thickness t, while the bending is cubic. Thus the smaller t is, the more expensive stretching deformations are compared with bending ones. Under compression a sheet will reduce its elastic energy by buckling into shapes that involve only small stretching deformations. Thus in many cases equilibrium shapes of thin sheets are based on zero stretching configurations.

The existence of bending energy (due to the finite sheet thickness) leads to the selection of the zero stretching configuration of minimum bending as a basis for the physical solution. The bending term acts as a perturbation on this configuration, smoothing it to form the energy minimum of the sheet [1]. In such a perturbative solution, the length scale that dominates the solution does not depend on the thickness of the sheet. In this paper, we will refer to this selection of equilibrium as the "small perturbation scenario." A confined slender rod is an example for such a mechanism. It buckles, and with decreasing thickness its shape converges to a buckled arc that preserves its rest length and fulfills the boundary conditions. The "wavelength" of the solution is determined by the boundary conditions and does not depend on the rod's thickness.

However, there are cases when boundary conditions exclude the existence of *any* smooth stretch-free configuration. In these cases a perturbative treatment is not applicable (since any stretch-free configuration would have an infinite bending energy) and a wavy equilibrium configuration is set by minimization of the full energy functional; we call this the "wrinkling scenario." The equilibrium configuration is characterized by the formation of the small scale structure with an explicit thickness dependence of the scaling. Examples are the wrinkling [2–4] and blistering [5–8] of constrained sheets.

Recently we observed that multiscale wavy structure can appear even on sheets that are *free* of any external constraint. We found that the edge of a torn plastic sheet can form a cascade of similar buckles over many length scales [9]. We proposed that the observed fractal structures correspond to the minimum of the elastic energy of sheets whose edges were stretched by the irreversible plastic deformations that accompanied the tearing. Further, we suggested that the same mechanism could describe other thin membranes such as leaves. In this view, symmetry breaking in growing thin membranes can result from the coupling between geometrical and mechanical properties of the tissue. Nechaev and Voituriez [10] have proposed a partially overlapping view. They have suggested that waviness of leaves appears when the leaves have a negative Gaussian curvature; however, their calculation was purely geometrical and did not involve an energy-based selection mechanism. Recent experiments [11,12] demonstrated that two-dimensional geometry is, indeed, important in leaf development and that leaf curvature can be tuned genetically [11]. However, no study has yet addressed the coupling between geometry and mechanics in leaves, and no quantitative study of the intrinsic geometry of leaves has been reported.

Several theoretical analyses motivated by our observations of multiscale wavy structures [9] have examined equi-

FIG. 1. A spade-shaped crack traveling in a polyethylene sheet that is pulled horizontally. The sheet edges created by the tearing have stable waves. y is the distance of a point from the edge, measured along the surface. The lines on the scale in the upper left corner are 1 mm apart.

libria of narrow elastic strips as a model problem [13,14]. Numerical studies of wide sheets by Marder *et al.* [15] and by Audoly and Boudaoud [16] obtained multiscale waves as energy minima of sheets with elongated edges. In [16] the authors studied the scaling of the shortest wavelengths in the cascades and proposed a resonancelike mechanism for the scaling of longer waves. They suggested that the observed wavy shapes are very close to existing smooth stretch-free configurations, perturbed by the bending energy of the sheet (the "small perturbation scenario"). This suggestion, however, has not been tested with experimental data.

In this paper we present and analyze measurements on torn plastic sheets and leaves. The experimental system is described in Sec. II, and the results are presented in Sec. III. We show that the process of tearing a thin plastic sheet leads to a hyperbolic equilibrium metric (i.e., a metric producing a negative Gaussian curvature) on the deformed part of the sheet, with an *increasingly negative* Gaussian curvature close to the edge. We present measurements of wavelengths and amplitudes of the waves and show that although the metrics are smooth and monotonic, a cascade is generated through a set of sharp transitions in which new modes emerge. Further, in Sec. III B we show that the scaling of wavelengths depends explicitly on the sheet thickness, as well as on the prescribed metric. This scaling leads to several predictions, one of which is that at vanishing thickness, sheets should form wrinkles with infinitesimal wavelengths *within the entire deformed region*, including at large distance from the edge. We argue that the observed scaling suggests, in contrast with [16], that the patterns are formed via a wrinkling scenario, and we describe a possible geometrical origin of the phenomenon. In Sec. III C we show how our ideas and techniques can be applied to a quantitative study of wavy leaves. The intrinsic metric of a leaf resembles that of the wavy plastic sheets, i.e., it is hyperbolic and depends mainly on the distance from the leaf's edge. The conclusions are presented in Sec. IV.

II. EXPERIMENTAL SYSTEM

Experiments are conducted on rectangular Teflon and polyethylene sheets (thickness 12–500 μm, 10–20 cm in x-y) that are pulled at a uniform rate on opposite sides, as illustrated in Fig. 1. The tearing generates a traveling spade-shaped crack. A resultant free sheet is then placed under a "Conoscan 3000" noncontact profilometer, and the sheet's

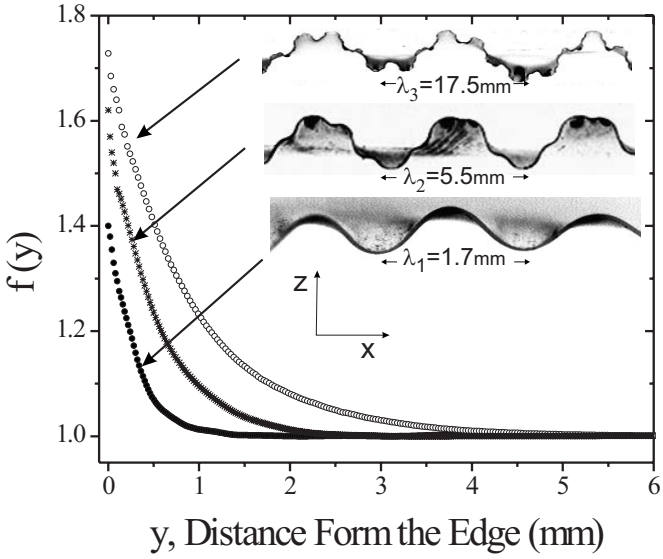

FIG. 2. Metric function describing the elongation in the x direction as a function of y, measured for 0.20-mm-thick polyethylene sheets for different conditions: top curve—crack velocity $v=0.5$ cm/s, steady state; middle—$v=5$ cm/s, steady state; bottom—$v=5$ cm/s, initial crack propagation. The resultant structures along the edge (inset) consists of three, two, and one generations, respectively.

profile $z(x,y)$ is obtained with a resolution of 25 μm in the x and y directions and 5 μm in the z direction. Next, y is redefined to be the distance of a point from the edge, measured along the surface.

III. RESULTS

A. Torn plastic sheets

Since the in-plane plastic deformation resulted from a steady propagation of the fracture tip, the deformation is invariant as a function of position x along the edge. This was confirmed by analyzing movies of the propagating tips and by the cutting experiment described in Sec. III B. Integration of the profile $z(x,y)$ at a fixed y provides the length of the sheet in the x direction. We call $f(y)$ the ratio of length at a given y to the length of the sheet prior to tearing. We show three examples of $f(y)$ in Fig. 2. The length element on the deformed surface is $dl^2=(fdx)^2+dy^2$, i.e., $f(y)$ is the xx component of the new equilibrium metric tensor produced by tearing the sheet. Although the sheets are deformed plastically *during* the tearing (when the stresses near the tip are dramatically enhanced), there is no reason to expect any additional plastic deformation *after* the tearing. Thus the relaxation of the deformed sheet is elastic.

The metric functions $f(y)$ approach unity far from the edge (where no plastic deformation has occurred) and increase convexly close to the edge. For the conditions of our experiments the amount of stretch at the edge $f(0)$ is less than 2 (see the examples in Fig. 2). Different experimental conditions (different materials, crack velocities, sheet dimensions) lead to different metric functions, reflecting the differ-

ent plastic deformation fields generated during the tearing. Typically we observe stable configurations consisting of 1, 2, and 3 generations of waves, as illustrated in the inset of Fig. 2. Patterns with up to six generations of similar waves were observed in 12-μm-thick sheets [9], but quantitative measurements were not possible for these sheets because of the low rigidity of such thin sheets.

In most cases the ratio of wavelengths of successive modes was found to be close to 3 and was the same for successive generations; that is, the patterns were self-similar. However, ratios up to 5 were observed, and the ratio between successive modes for a given sheet in some cases changed for different generations. These observations are in accord with [16], where ratios of 3 and 5 were shown to be energetically favorable in self-similar cascades.

Since equilibrium configurations of thin sheets involve very small stretching deformations, we start by considering the properties of isometrics, i.e., sheets with no stretching. What can be said about the shapes of unstretched surfaces that have *exactly* the metric prescribed by the tearing? The celebrated *Theorema Egregium* by Gauss shows that the local Gaussian curvature on a surface $K(x,y)$ (the product of the principal curvatures) is set by the local metric coefficients and becomes in our case (see, e.g., [17])

$$K(y) = -\frac{1}{f}\frac{d^2 f}{dy^2}. \tag{1}$$

Since f is convex, $K<0$ over the entire deformed zone. Thus configurations with no stretching have everywhere saddlelike points and a free sheet must "spontaneously" buckle out of the plane to adopt this curvature, even without any constraints on the boundaries. The Gaussian curvature is invariant with respect to x, but Eq. (1) does not tell us why equilibrium configurations would involve a repetitive breakdown of the translation symmetry in the x direction.

The height of the surface $z(x,y)$ as a function of x at different distances y from the edge of a plastic sheet is shown in Fig. 3(a). We Fourier transform the spatial profiles to obtain wave number spectra such as those in Fig. 3(b). Graphs of the mode amplitudes versus y [Fig. 3(c)] reveal transitions at which modes of shorter and shorter wavelength are added towards the edge; these transitions are not discernible in graphs of $f(y)$. Three modes are distinguishable in Figs. 3(b) and 3(c) [18]. In the next section we examine the scaling of the wavelengths.

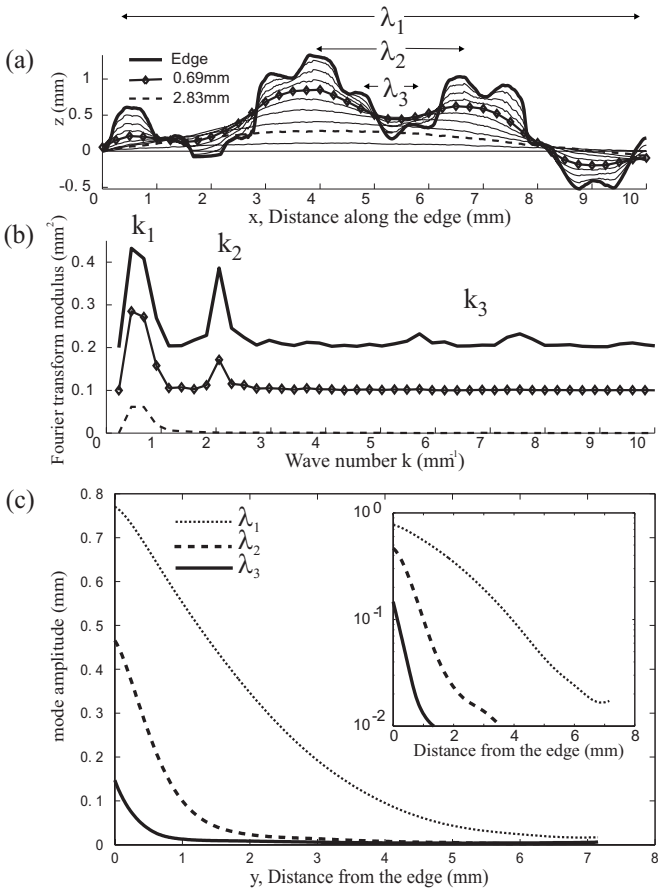

FIG. 3. The emergence of different modes in the cascade as a function of the distance y from the edge of a 0.25-mm-thick polyethylene sheet. (a) The amplitude $z=f(x,y)$ along lines of increasing distance y from the edge (measured along the surface): 0, 0.16, 0.34, 0.52, 0.69, 0.96, 1.41, 2.12, 2.83, and 4.43 mm. (b) Power spectra for measurements in (a) at distances 0, 0.69, and 2.83 mm, obtained from the full sample of 30 mm length (the spectra are shifted vertically with respect to one another for visualization; $k=\frac{2\pi}{\lambda}$). The spectra reveal a long wavelength mode [only a single wavelength of this mode is shown in (a)] at large y and smaller wavelength modes closer to the edge. The shortest mode is split into two side bands because it is a modulation of a curved base line generated by the larger modes (see text). (c) Normalized amplitudes of the modes, which appear in (b), as a function of the distance y from the edge.

B. Wavelength scaling

Structures that are based on a stretch-free wavy configuration could depend only on properties of the metric. Thus, wavelengths would be set by the "geometrical" length scale given by $f(y)$. In this case, there should not be an explicit dependence of long wavelengths on the thickness, which could enter only as a cutoff for the shortest possible wavelength. However, if the cascades are formed through a wrinkling scenario, the sheet thickness t will explicitly affect all wavelengths, including the long ones.

To test whether wavelengths at locations away from the edge were set by local properties of the sheet, narrow strips were cut off a torn sheet. The result was that the amplitude and wavelength of the remaining sheet scarcely changed, even when the cutting was done repeatedly (Fig. 4). This demonstrates dramatically that wavelengths are selected by the *local* properties of a sheet.

The local length scale $L(y)$ for wavelength selection should be a combination of a geometrical local length scale $L_{geo}(y)$ and the local thickness $t(y)$. To explore the dependence on t, we conjecture a scaling relation with an adjustable scaling exponent α,

$$\lambda(y) \propto L_\alpha(y) = t^\alpha(y) L_{geo}^{1-\alpha}(y). \tag{2}$$

An exponent $\alpha=0$ would imply that the thickness is not a relevant length scale and wavelengths are determined solely

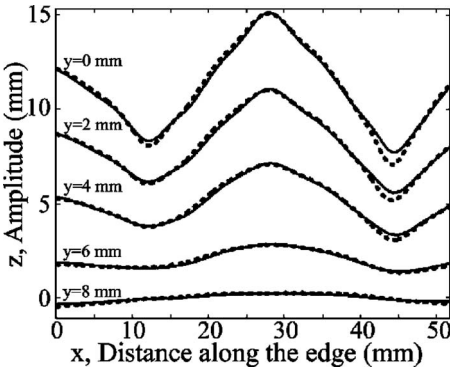

FIG. 4. Comparison of the amplitude as a function of x at different y for the full sheet (solid lines) with the amplitude measured after cutting off successive strips of 3 mm along the edge (dotted lines). The comparison shows that the wavelengths and amplitudes are not affected by the removal of the strips. The values of y were measured here in the laboratory frame with respect to the cut edge, rather than along the surface as in the rest of the measurements we present.

by $f(y)$, while $\alpha=1$ would imply that wavelengths do not depend on the metric, but only on the thickness. We look for a value of α that would collapse the data onto a single curve. Several comments are appropriate regarding the proposed scaling relation:

(1) Our measurements show that the sheet thickness decreases towards the edge, with a maximum measured decrease of 60% (while the full range of local sheet thickness over the entire data set spans more than one order of magnitude). Since both the metric and the sheet thickness vary continuously with y, $L(y)$ must also be a continuous function of y. On the other hand, the observed wavelengths remain fixed, and new wavelengths emerge at smaller y. Thus, any assignment of a local length scale to a mode is somewhat arbitrary. Despite this difficulty, our analysis aims to determine how the scaling of the *entire pattern* depends on the thickness.

(2) The natural geometrical length scale L_{geo} at a distance y from the edge is the inverse geodesic curvature that is prescribed by the metric along lines $y=constant$; L_{geo} is an intrinsic property in the sense that it is determined solely by the metric and conserved under bending of a sheet. We determine L_{geo} by cutting narrow strips parallel to a sheet's buckled edge and flattening them between glass plates, as illustrated in Fig. 5. A strip curls into an arc or ring whose radius is L_{geo}. Expressing the geodesic curvature with the coefficients of the prescribed metric yields $L_{geo}(y)=\frac{f(y)}{f'(y)}$. In our sheets L_{geo} is typically of order 1 mm on the edge, and increases to values of order 1 m away from the edge, as shown in Fig. 6.

(3) The distance from the edge y corresponding to a given mode in the cascade is taken to be midway between its onset and that of the onset of the next one. Changing the definition of y to be the onset of the next mode hardly affected the resultant scaling.

The scaling given by Eq. (2) implies $\frac{\lambda(y)}{t(y)}=\left(\frac{f(y)}{f'(y)t(y)}\right)^{1-\alpha}$. To test whether our data are described by such scaling, we plot

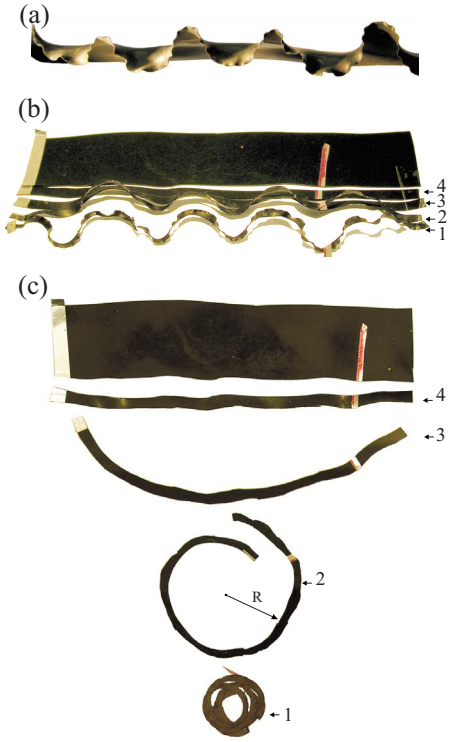

FIG. 5. (Color online) The intrinsic geometry of a buckled sheet is revealed by flattening thin strips cut parallel to the buckled edge; a flattened strip curls into an arc or ring whose radius of curvature is L_{geo}. (b) Four narrow strips of equal width cut successively from the edge of the sheet. (c) Flattened strips obtained at different distances from the edge, illustrating the increase in radii of curvature with increasing distance from the edge. The local curvature along each strip is the local geodesic curvature along the cut. The lines on the right were taped onto the sheet prior to cutting, to aid in visualization and orientation.

$\frac{\lambda(y)}{t(y)}$ versus $\frac{f(y)}{f'(y)t(y)}$ for data from all modes and sheet thicknesses. Figure 7 shows that the data are well described by

$$\lambda(y) \propto t(y)^{0.3}\left(\frac{f(y)}{f'(y)}\right)^{0.7}. \tag{3}$$

A least squares fit of the data to a line yields $\alpha=0.31\pm0.03$. The exponent α may well depend on f; its value is not universal.

The result in Fig. 7 suggests that the thickness is a relevant length scale in determining wavelengths at all scales. Thus the observations support the wrinkling scenario rather than the small perturbation scenario. The decrease of $\frac{f(y)}{f'(y)}$ as $y\to0$ (Fig. 6) leads to shorter and shorter wavelength modes as the edge is approached. In contrast, an exponential $f(y)$ would result in a single wavelength, as has been demonstrated by numerical simulations by Marder [15], who also found from simulations that a $f(y)$ given by a sum of several exponential terms or given by a power law yields a cascade of waves.

The explicit thickness dependence of λ has an important consequence: if a sheet with a given metric has a thickness

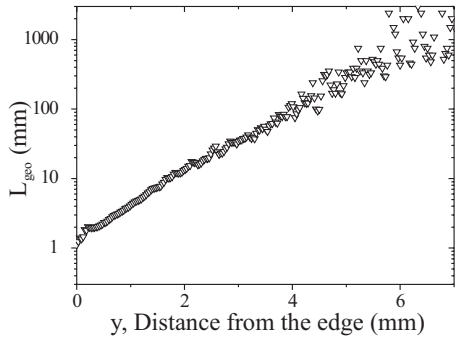

FIG. 6. The geodesic radius of curvature L_{geo} for a 0.2-mm-thick polyethylene sheet, as a function of distance from the edge. L_{geo} was computed from $L_{geo}=\frac{f(y)}{f'(y)}$, where $f'(y)$ was obtained by numerical differentiation of $f(y)$ for 0.1 mm intervals, for three generations of waves (see Fig. 2). The values of L_{geo} would correspond to the radii of curvature of strips if they were cut from the sheet like those in Fig. 5(c). Far from the edge L_{geo} is much larger than the largest observed wavelength, while near the edge the length decreases exponentially, leading to the generation of the short wavelengths of the buckled sheet. The decrease in L_{geo} is a significant difference between our sheets and the hyperbolic plane, where L_{geo} is constant.

that approaches zero, the sheet will wrinkle *everywhere* at wavelengths that are vanishingly small. Even a relatively flat sheet where L_{geo} is large will develop wrinkles at short wavelengths, provided that its thickness is small enough. As the ratio between L_{geo} and t increases, the wavy pattern will consist of short waves that are flat in the y direction, i.e., the principal curvature in the x direction at the tops of ridges will be much larger than in the y direction along the tops of ridges. This difference between principal curvatures increases as the thickness decreases, in contrast with the "perturbation scenario," where the principal curvatures would be

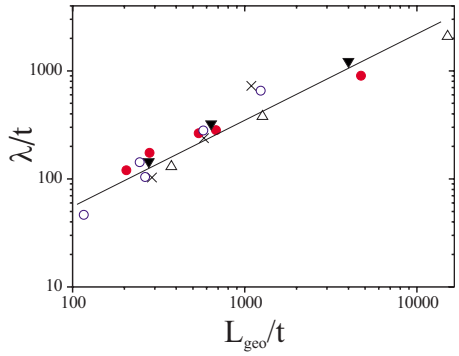

FIG. 7. (Color online) The wavelength λ of the waves as a function of the geometric length scale L_{geo}, where both lengths are normalized by the local sheet thickness t. The data for wave modes of different generations and for sheets of different thicknesses all collapse onto a single line that has slope 0.7, which implies $\lambda(y) \propto t(y)^{0.3}\left(\frac{f(y)}{f'(y)}\right)^{0.7}$. $\lambda(y)$, $t(y)$, and $f'(y)$ were evaluated at a distance y from the edge chosen to be in the middle between the onset of a mode and the onset of the next shorter mode. The sheet thicknesses were open circles: 508 μm; solid circles: 203 μm; crosses: 255 μm; solid triangles: 100 μm.

as close to each other as possible in order to minimize the bending energy.

The scaling in Eq. (3) resembles the wavelength scaling in flat sheets that are wrinkled under confinement, which excludes the existence of a smooth, stretch-free, configuration [2,3]. However, there is an important difference between our system and the ones studied in [2,3]: our sheets are free, not subjected to any constraint. How does a free sheet come to be wrinkled, a behavior that results from confinement? We propose that the wrinkling arises because there is no smooth embedding of sheets with the prescribed metrics in Euclidean space: any mathematical sheet that obeys *exactly* the distribution of distances prescribed by the tearing, and is flat at a large distance from the edge, must include regions with infinite curvature. Thus, any physical sheet with this metric will have infinite bending energy, no matter how thin it is. A perturbative treatment, based on an isometry, is thus not applicable, and the entire energy functional must be minimized simultaneously. The different thickness dependence of the stretching and bending terms leads to an explicit thickness dependence of the characteristic length scales.

Indeed, the embedding of hyperbolic metrics is far from trivial. Hilbert proved in 1901 that the embedding of the entire hyperbolic plane (a surface with a constant Gaussian curvature $K=-1$) in three-dimensional Euclidean space cannot be smooth [19] (a refined proof is given in [20]). Explicit embeddings that were constructed involved singularities [10] or an infinitely small structure [21]. Our finite-sized sheets differ from the hyperbolic plane in that they have larger and larger negative curvature towards their edges (Fig. 5) and become completely flat far from their edges. We are not familiar with mathematical work that addresses embedding of such surfaces. Our data suggest that such metrics do not have any embedding that involves only long wavelengths. In this case, our free sheets are "confined" by the Euclidean space itself and respond by forming wrinkled structures.

C. Application to leaves

In this section the goal is to determine whether the shapes of wavy leaves can result from an enhanced growth near their edges, i.e., do some wavy leaves have essentially uniform growth parallel to their edge? We analyze leaves in the same way as the buckled plastic sheets in Fig. 5. Narrow strips of constant width are cut parallel to the edge of a leaf and then flattened to determine the geodesic curvature along lines $y=constant$ (Fig. 8). Measurements on a wavy bay leaf reveal a geometry similar to that of the torn plastic sheets: the radius of the strips decreases as the edge is approached [Fig. 8(b)], indicating negative curvature. In contrast, for a flat leaf [Fig. 8(a)] the radius increases towards the edge. Just as for the plastic sheets, we find for a wavy leaf that the geodesic curvature at a given y is nearly constant—features on the leaf such as the system of veins or the leaf's waviness hardly affect $f(y)$. We conclude that uniform growth along the edge of a leaf could lead to waviness, and the length scales could be set by elasticity and geometry rather than by explicit genetic encoding.

Since we find the metric of a leaf to be nearly independent of x and to depend strongly on y, we can apply our method

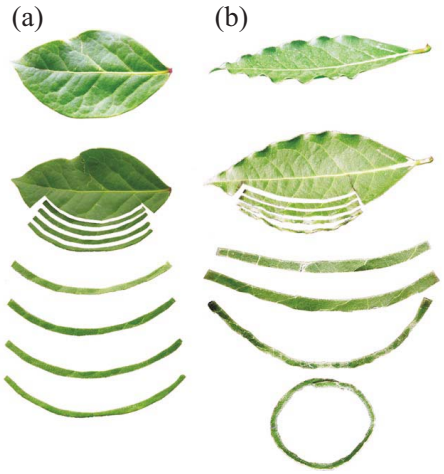

FIG. 8. (Color online) The intrinsic geometry of a leaf is determined for (a) flat and (b) wavy leaves (from the same bay tree) by the same method used in determining the properties of the torn plastic sheet (Fig. 5). Four narrow strips of equal width are cut successively from the edge of the leaf and are flattened between two glass plates; the flattened strips curl into arcs or rings whose radii of curvature is L_{geo}. In the flat leaf L_{geo} increases towards the edge, while in the wavy leaf it decreases. In both cases L_{geo} is *nearly constant* along the edge. This indicates that the metric of the leaf depends mainly on the distance from the edge (from [12]).

for determining $f(y)$ in plastic sheets to a leaf (Fig. 9). The resultant $f(y)$ is shown in Fig. 9(c). Since the leaf edge is curved, we use locally a polar rather than Cartesian coordinate system. In this coordinate system a flat surface has a linearly increasing metric function $f(y)$ [the Gaussian curvature associated with a linear $f(y)$ is zero]. We have determined $f(y)$ for many wavy leaves from different plants, such as Wisteria floribunda, Laurus nobilis (Bay leaf) and Lemonwood (Pittosporum eugenioides). In all leaves we have measured a linear increase in $f(y)$ in the flat region far from the edge and a convex $f(y)$ that increases as the leaf edge is approached.

Our results demonstrate that profilometer scans of wavy leaves can yield both their two-dimensional metric and their shape in space. Future work should examine whether the observed wavy shapes minimize the energy of an elastic sheet with the measured metric. Such an analysis will indicate when a measured metric suffices to explain the waves in a leaf, and when other mechanisms are required. While such analysis is left for the future, we mention recent work that demonstrated that when the genetic control of the distribution of in-plane tissue production was perturbed, the leaves that grew were distorted and wrinkled [11].

IV. CONCLUSIONS

Our measurements on torn plastic sheets show that different hyperbolic metrics formed during the tearing lead to different multiscale wavy structures. Away from the edge we find long wavelengths and then, as the edge is approached, shorter and shorter wavelength modes emerge at well defined distances from the edge and are superimposed upon one another. We have shown that the wavelengths in the patterns are selected locally and depend on both the sheet thickness t and a geometrical length scale L_{geo}, which we computed from measurements of the metric function $f(y)$: $L_{geo}=f/f'$. The wavelength was found to scale as $\lambda \propto t^{0.3} L_{geo}^{0.7}$; thus for $t \to 0$, $\lambda \to 0$. This scaling indicates that the embedding in Euclidean space of a sheet with the measured metrics must involve infinitely small structure. Finally, we have shown that the geometry of wavy leaves is similar to that of the wavy plastic sheets and can be analyzed in a similar manner. We have performed the first quantitative measurements of the metrics and wavelengths of leaves. This work opens the way for future studies of spontaneous wrinkling in growing sheets in nature.

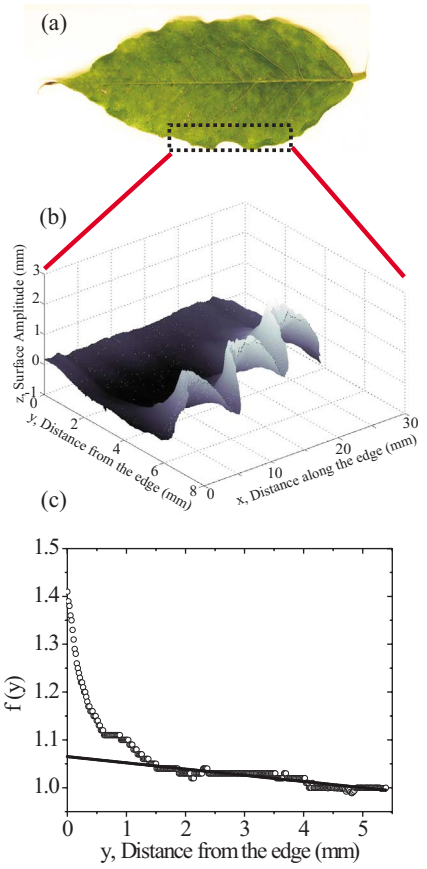

FIG. 9. (Color online) A wavy leaf of Wisteria (a) is scanned with a noncontact profilometer to obtain the profile in (b), which is used to obtain the metric function $f(y)$ in (c). This function is compared with $f(y)$ for a flat sheet with the same contour (solid line), which is linear, thus not generating Gaussian curvature. The difference between the two functions $f(y)$ yields the excess length in the wavy leaf compared to the flat leaf.

ACKNOWLEDGMENTS

We thank M. Marder, S. Smith, L. Sadun, and S. Venkataramani for helpful discussions. This work was supported by the Office of Naval Research and the Sid Richardson

Foundation. E.S. acknowledges support of the Fulbright Foundation, ISF—Bikura and GIF. B.R. acknowledges the support of CIMAT, CONICYT (Postdoctorado Grant No. FONDECYT 3010001), and the French Ministry of Research ACI funding.

[1] A. Pogorelov, *Bending of Surfaces and Stability of Shells* (American Mathematical Society, Providence, 1988).
[2] E. Cerda, K. Ravi-Chandar, and L. Mahadevan, Nature (London) **419**, 579 (2002).
[3] E. Cerda and L. Mahadevan, Phys. Rev. Lett. **90**, 074302 (2003).
[4] K. Efimenko, M. Rackaitis, E. Manias, A. Vaziri, L. Mahadevan, and J. Genzer, Nat. Mater. **4**, 293 (2005).
[5] M. Ortiz and G. Gioia, J. Mech. Phys. Solids **42**, 531 (1994).
[6] H. Ben Belgacem, S. Conti, A. DeSimone, and S. Muller, J. Nonlinear Sci. **10**, 661 (2000).
[7] W. Jin and R. V. Kohn, J. Nonlinear Sci. **10**, 355 (2000).
[8] H. Ben Belgacem, S. Conti, A. DeSimone, and S. Muller, Arch. Ration. Mech. Anal. **164**, 1 (2002).
[9] E. Sharon, B. Roman, M. Marder, G. S. Shin, and H. Swinney, Nature (London) **419**, 579 (2002).
[10] S. Nechaev and R. Voituriez, J. Phys. A **34**, 11069 (2001).
[11] U. Nath, B. Crawford, R. Carpenter, and E. Coen, Science **299**, 1404 (2003).
[12] E. Sharon, M. Marder, and H. L. Swinney, Am. Sci. **92**, 254 (2004).
[13] M. Marder, Found. Phys. **33**, 1743 (2003).
[14] B. Audoly and A. Boudaoud, C. R. Mec. **330**, 1 (2002).
[15] M. Marder, E. Sharon, B. Roman, and S. Smith, Europhys. Lett. **62**, 498 (2003).
[16] B. Audoly and A. Boudaoud, Phys. Rev. Lett. **91**, 086105 (2003).
[17] A. V. Pogorelov, *Differential Geometry* (P. Noordhoff nv, Groningen, The Netherlands, 1956).
[18] In power spectra of profiles $z(x,y)$, such as in Fig. 3(b), peaks corresponding to higher modes appear less and less well defined. These modes are not periodic with respect to the lab's x coordinate but are periodic modulations of the curved base line formed by the longer wavelengths, on which they are superimposed. Therefore, we obtain the amplitude of a given mode A_n, by comparing two profiles: The first—the "base line"—is the surface profile at a given y that consists of modes of lower order than n [obtained by filtering $i \geq n$ modes out of $z(x)$]. The second is the same profile with the nth mode (obtained by filtering out all $i > n$ modes). The root mean square of distances between the two curves (measured perpendicularly to the local tangent to the "base line") gives the amplitude when divided by $\sqrt{2}$.
[19] D. Hilbert, Trans. Am. Math. Soc. **2**, 87 (1901).
[20] N. V. Efimov, Mat. Sb. **64**, 286 (1964).
[21] N. H. Kuiper, Proc. K. Ned. Akad. Wet., Ser. A: Math. Sci. **58**, 683 (1955).